Available online at www.sciencedirect.com
ScienceDirect
Applied Soft Computing 8 (2008) 30–45
Applied Soft Computing
www.elsevier.com/locate/asoc

An immunological approach to mobile robot reactive navigation

Guan-Chun Luh *, Wei-Wen Liu

Department of Mechanical Engineering, Tatung University, Taipei, Taiwan, ROC

Received 22 August 2005; received in revised form 8 August 2006; accepted 31 October 2006
Available online 11 December 2006

Abstract

In this paper, a reactive immune network (RIN) is proposed and employed for mobile robot navigation within unknown environments. Rather than building a detailed mathematical model of artificial immune systems, this study tries to explore the principle in an immune network focusing on its self-organization, adaptive learning capability, and immune feedback. In addition, an adaptive virtual target method is integrated to solve the local minima problem in navigation. Several trapping situations designed by the early researchers are adopted to evaluate the performance of the proposed architecture. Simulation results show that the mobile robot is capable of avoiding obstacles, escaping traps, and reaching the goal efficiently and effectively.

Keywords: Artificial immune system; Mobile robot navigation; Reactive immune network; Adaptive virtual target method; Local minima problem

1. Introduction

Autonomous mobile robots have a wide range of applications in industries, hospitals, offices, and even the military, due to their superior mobility. Some of their capabilities include automatic driving, intelligent delivery agents, assistance to the disabled, exploration and map generation for environmental cleanup, etc. In addition, their capabilities also allow them to carry out specialized tasks in environments inaccessible or very hazardous for human beings such as nuclear plants and chemical handling. They are also useful in emergencies for fire extinguishing and rescue operations. Combined with manipulation abilities, their capabilities and efficiency will increase and can be used for dangerous tasks such as security guard, exposition processing, as well as undersea, underground and even space exploration.

In order to adapt the robot's behavior to any complex, varying and unknown environment without further human intervention, intelligent learning algorithms have been successively adopted to develop the behavior-based intelligent mobile robots. Intelligent mobile robots should be able to extract information from the environment, use their built-in knowledge to perceive, act and adapt within the environment. They move and plan their actions to accomplish objectives defined either extrinsically by a human programmer or intrinsically on the basis of a general objective of survival. As a result, path planning of intelligent robot behavior plays an important role in the development of flexible automated systems. The design goal for path planning is to enable a mobile robot to navigate safely and efficiently without collisions to a target position in an unknown and complex environment. The navigation strategies of mobile robots can be generally classified into two categories, global path planning and local reactive navigation. The former such as artificial potential fields [1], connectivity graphs or cell decomposition [2] is done offline, and the robot has complete prior knowledge about the shape, location, orientation, and even the movements of the obstacles in the environment. Its path is derived utilizing some optimization techniques to minimize the cost of the search. However, it has difficulty handling a modification of the environment, due to some uncertain environmental situations, and the reactive navigation capabilities are indispensable since the real-world environments are apt to change over time. On the other hand, local reactive navigation employing some reactive strategies to perceive the environment based on the sensory information and path planning is done online. The robot has to acquire a set of stimulus–action mechanisms through its sensory inputs, such as distance information from infrared sensors, visual information from

* Corresponding author. Tel.: +886 2 25925252x3410x806; fax: +886 2 25997142.
E-mail address: gluh@ttu.edu.tw (G.-C. Luh).

1568-4946/$ – see front matter
doi:10.1016/j.asoc.2006.10.009

cameras or processed data derived after appropriate fusion of numerous sensor outputs. The action taken by the robot is usually an alternation of steering angle and/or translation velocity to avoid collisions and reach the desired target. Nevertheless, it does not guarantee a solution for the mission, nor is the solution the optimal one.

Reactive behavior-based mobile robot responds to stimuli from the dynamic environment, and its behaviors are guided by local states of the world. Its behavior representation is situated at a sub-symbolic level that is integrated into its perception-action (*i.e.*, sensor-motor) capacities analogous to the manifestation of the reflex behavior observed in biological systems. Some researches have focused on this kind of robot system and have demonstrated its robustness and flexibility against an unstructured world [3,4]. Reactive behavior-based strategy is now becoming attractive in the field of mobile robotics [5] to teach the robot to reach the goal and avoid obstacles. However, a well-known drawback of reactive navigation is that the mobile robot suffers from local minima problems in that it uses only locally available environmental information without any previous memory. In other words, a robot may get trapped in front of an obstacle or wander indefinitely in a region whenever it navigates past obstacles toward a target position. This happens particularly if the environment consists of concave obstacles, mazes, etc. Several trap escape algorithms, including the random walk method [3], the multi-potential field method (MPF) [4], the tangent algorithm [5], the wall-following method [6,7], the virtual obstacle scheme [8,9], and the virtual target approach [10,11], have been proposed to solve the local minima problems. In the case of the random walk method, numerous random decisions are made when a trap is detected. As to the MPF approach, several potential fields are implemented and selected randomly in the local minima situations. In the wall-falling approach, the action is switched between potential field-based behavior and wall-following behavior. However, this method is likely to generate new local minima. In the virtual obstacle scheme, a virtual obstacle is generated around a local minima point and creates as extra force to repel the robot from it. A lot of memory is required, however, for storing all the locations that the robot has previously visited. Therefore, this scheme is very inefficient. In the virtual target approach, the target is switched to a virtual location in the partial segment of the possible limit cycle path and is very effective in a simple U-shaped trap situation. Nevertheless, it failed to escape from recursive U-trapping situations that may arise when the robot experiences a new trap while approaching the virtual target, and thus a virtual-target-side concept [12] was proposed to circumvent the trapping situation.

In the last decade, it has been shown that the biologically inspired artificial immune system (AIS) has a great potential in the fields of machine learning, computer science and engineering [13–16]. Dasgupta [13] summarized that the immune system has the following features: self-organizing, memory, recognition, adaptation, and learning. There are a lot of researches investigating the interactions between various components of the immune system or the overall behaviors of the systems based on an immunological point of view. Immunized systems consisting of agents (immune-related cells) may have adaptation and learning capabilities similar to artificial neural networks, except that they are based on dynamic cooperation of agents [17]. Moreover, immune systems provide an excellent model of adaptive process operating at the local level and of useful behavior emerging at the global level [13,18]. Accordingly, the artificial immune system can be expected to provide various feasible ideas for the applications of mobile robots [19–33]. Hart et al. [19] proposed a role for immunology in ‘‘next generation’’ robot controllers. They have sketched out a line of work, both in terms of studying robot development and AIS. Ishiguro and his colleagues [20–23] proposed an immune-network based decentralized, consensus-making mechanism and confirmed the validity by applying to predator-food and garbage-collecting problems, respectively. In addition, two adaptation mechanisms, adjustment and innovation, were developed to improve the performance. Simulations and real experiments were utilized to confirm the validity of the proposed architecture. Later, Michelan and Von Zuben [24] proposed an evolved artificial immune network for garbage collection problem. The immune network idiotopes were evolved using a genetic algorithm. The simulation results illustrated that the evolved immune network is more robust and flexible compared with those proposed in [20–23]. Luh and Cheng [18] applied an immunized reinforcement adaptive learning mechanism to an intelligent mobile robot and evaluated using a ‘‘food foraging work’’ problem. In addition, immune networks have been applied to distributed autonomous robotics system problems [25,26]. Meshref and VanLandingham [25] utilized immune network to solve dog and sheep problem while Duan et al. [26] employed immune network for predator and prey (*i.e.* path finding and cooperation) problem. Furthermore, immunology-based algorithms were implemented for multi-robot cooperative problem [27–29]. In [27], Thayer and Singh developed IDARA (immunology-derived distributed Autonomous Robotics Architecture) for applications in large-scale, heterogeneous multi-robot team.

As to mobile robot navigation problem, Ishiguro et al. [30] proposed a two-layer (situation-oriented and goal-oriented) immune network to behavior control of autonomous mobile robots. Simulation results show that mobile robot can reach goal without colliding fixed or moving obstacles. Later, Lee et al. [31] constructed obstacle-avoidance and goal-approach immune networks for the same purpose. The results present more than 70% of the reaching probability on the usage of the artificial immune network. Additionally, it shows the advantage of not falling into a local loop. Afterward, Vargas et al. [32] developed an Immuno-Genetic Network for autonomous navigation. It has the immune network implementing a dynamic process of decision-making, and the evolutionary algorithm defining network structure. The simulations show that the evolved immune network is capable of correctly coordinating the system towards the objective of the navigation task. In addition, some preliminary experiment on a real

Khepera II robot demonstrated the feasibility of the network. Recently, Duan et al. [33] proposed an immune algorithm for path planning of a car-like wheeled mobile robot. Simulations indicate that the algorithm can finish different tasks within shorter time. It should be noted that, however, all of the above researches did not consider solving the local minima problems. Besides, their structures of antibody defined (binary-type of paratope, action, and idiotype) is much complex than that (action) in this study.

A reactive immune network navigation mechanism for mobile robots is constructed in this study. The application task for the mobile robot is to navigate in an unknown and complex environment while avoiding static obstacles but reaching a goal safely. The basic concept of the proposed scheme is described in the following sections. The related biological immune system is described in Section 2, whereas Section 3 presents the developed methodology of RIN in detail. Section 4 illustrates the effectiveness of the proposed methodology through some simulations. Finally, Section 5 concludes the paper.

2. How biological immune system works

The immune system protects living organisms from foreign substances such as viruses, bacteria, and other parasites (called antigens). The body identifies invading antigens through two inter-related systems: the innate immune system and the adaptive immune system. A major difference between these two systems is that adaptive cells are more antigen-specific and have greater memory capacity than innate cells. Both systems depend upon the activity of white blood cells where the innate immunity is mediated mainly by phagocytes, and the adaptive immunity is mediated by lymphocytes as summarized in Fig. 1. The phagocytes possess the capability of ingesting and digesting several microorganisms and antigenic particles on contact. The adaptive immune system uses lymphocytes that can quickly change in order to destroy antigens that have entered the bloodstream. Lymphocytes are responsible for the recognition and elimination of the antigens. They usually become active when there is some kind of interaction with an antigenic stimulus leading to the activation and proliferation of the lymphocytes. Two main types of lymphocytes, namely B-cells and T-cells, play a remarkable role in both immunities [34]. Both B-cell and T-cell express in their surfaces antigenic receptors highly specific to a given antigenic determinant. The former takes part in the humoral immunity and secrete antibodies by the clonal proliferation while the latter takes part in cell-mediated immunity. One class of the T-cells, called the Killer T-cells, destroys the infected cell whenever it recognizes the infection. The other class that triggers clonal expansion and stimulates or suppresses antibody formation is called the Helper T-cells.

When an infectious foreign pathogen attacks the human body, the innate immune system is activated as the first line of defense. Innate immunity is not directed in any way towards specific invaders but against any pathogens that enter the body. It is called the non-specific immune response. The most important cell in innate immunity is a phagocyte, which internalizes and destroys the invaders to the human body. Then the phagocyte becomes an Antigen Presenting Cell (APC). The APC interprets the antigen appendage and extracts the features by processing and presenting antigenic peptides on its surface to the T-cells and B-cells. These lymphocytes will be able to sensitize this antigen and be activated. Then the Helper T-cell releases the cytokines that are the proliferative signals acting on the producing B-cell or remote the other cells. On the other hand, the B-cell becomes stimulated and creates antibodies when it recognizes an antigen. Recognition is achieved by inter-cellular binding, which is determined by molecular shape and electrostatic charge. The secreted antibodies are the soluble receptor of B-cells and these antibodies can be distributed throughout the body [35]. An antibody's paratope can bind an antigen's epitope according to its affinity. Moreover, B-cells are also affected by Helper T-cells during the immune responses [36]. The Helper T-cell plays a remarkable key role for deciding if the immune system uses cell-mediated immunity (by Th1

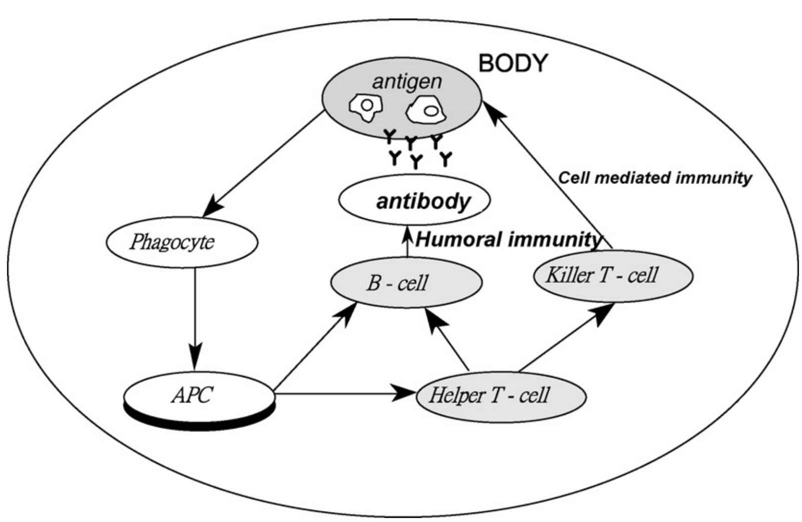

Fig. 1. Illustration of the biological immune system.

Helper T-cells) or humoral immunity (by Th2 Helper T-cells) [34], and it connects the non-specific immune response to make a more efficient specific immune response. The Helper T-cells work primarily by secreting substances known as cytokines and their relatives [34] that constitute powerful chemical messengers. In addition to promoting cellular growth, activation and regulation, cytokines can also kill target cells and stimulated macrophages.

The immune system produces the diverse antibodies by recognizing the idiotype of the mutual receptors of the antigens between antigen and antibodies and between antibodies. The relation between antigens and antibodies and that amongst antibodies can be evaluated by the value of the affinity. In terms of affinities, the immune system self-regulates the production of antibodies and diverse antibodies. Affinity maturation occurs when the maturation rate of a B-cell clone increases in response to a match between the clone's antibody and an antigen. Those mutant cells are bound more tightly and stimulated to divide more rapidly. Affinity maturation dynamically balances exploration versus exploitation in adaptive immunity [37]. It has been demonstrated that the immune system has the capability to recognize foreign pathogens, learn and memorize, process information, and discriminate between self and non-self [34,37]. In addition, the system can be maintained even faced with a dynamically changing environment.

Jerne [38] has proposed the idiotypic network hypothesis (immune network hypothesis) based on mutual stimulation and suppression between antibodies as Fig. 2 illustrates. This hypothesis is modeled as a differential equation simulating the concentration of a set of lymphocytes. The concept of an immune network states that the network dynamically maintains the memory using feedback mechanisms within the network. The various species of lymphocytes are not isolated but communicate with each other through the interaction antibodies. Jerne concluded that the immune system is similar to the nervous system when viewed as a functional network. Based on his speculation, several theories and mathematical models have been proposed [39–43]. In this study, the dynamic equation proposed by Farmer et al. [40] is employed as a reactive immune network to calculate the variation on the concentration of antibodies, as shown in the following equations:

$$\frac{\mathrm{d}A_i(t)}{\mathrm{d}t} = \left(\sum_{\ell=1}^{N_{\mathrm{Ab}}} m_{i\ell}^{\mathrm{st}} a_\ell(t) - \sum_{k=1}^{N_{\mathrm{Ab}}} m_{ki}^{\mathrm{su}} a_k(t) + m_i - k_i\right) a_i(t) \tag{1}$$

$$a_i(t) = \frac{1}{1+\exp(0.5 - A_i(t))} \tag{2}$$

where i, ℓ, $k = 0, 1, \ldots, N_{\mathrm{Ab}}$ are the subscripts to distinguish the antibody types and N_{Ab} is the number of antibodies. A_i and a_i are the stimulus and concentration of the ith antibody. m_{ij}^{st}, m_{ki}^{su} indicate the stimulative and suppressive affinity between the ith and the jth, kth antibodies, respectively. m_i denotes the affinity of antigen and antibody i, and k_i represents the natural death coefficient. Eq. (1) is composed of four terms. The first term shows the stimulation, while the second term depicts the suppressive interaction between the antibodies. The third term is the stimulus from the antigen, and the final term is the natural extinction term, which indicates the dissipation tendency in the absence of any interaction. Eq. (2) is a squashing function to ensure the stability of the concentration [23].

3. Reactive immune network

A reactive immune network inspired by the biological immune system for robot navigation (goal-reaching and obstacle-avoidance) is described in this section. It implies using a combination of both the prior behavior-based information and an on-line adaptation mechanism based on the features of the immune system. The architecture of the proposed navigation system is depicted in Fig. 3. The antigen's epitope is a situation detected by sensors and provides the information about the relationship between the current location and the obstacles, along with the target. This scene-based

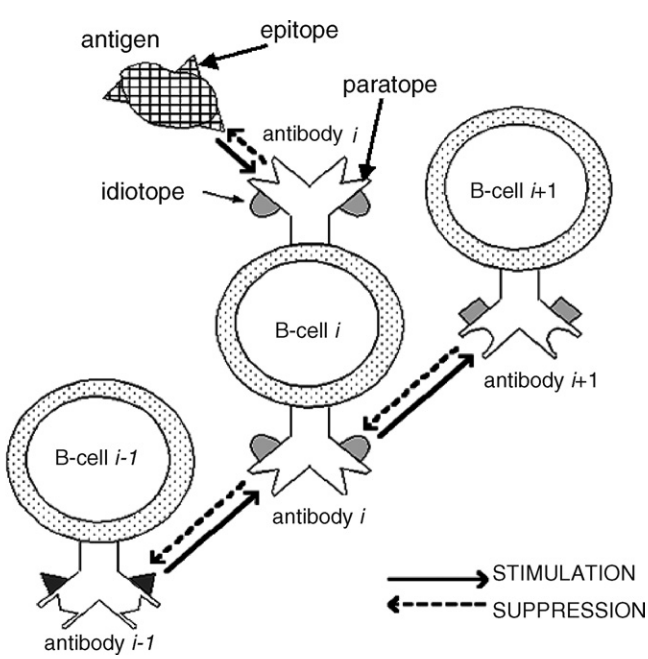

Fig. 2. Idiotypic network hypothesis.

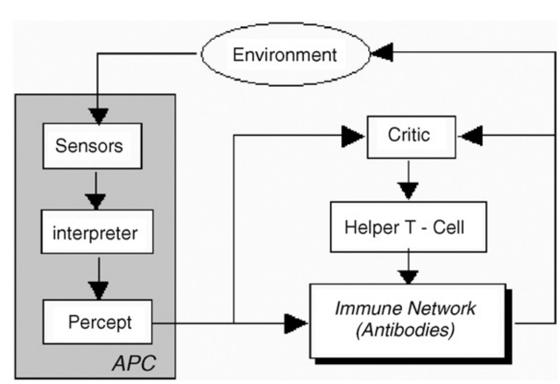

Fig. 3. The architecture of the immunized network reactive system.

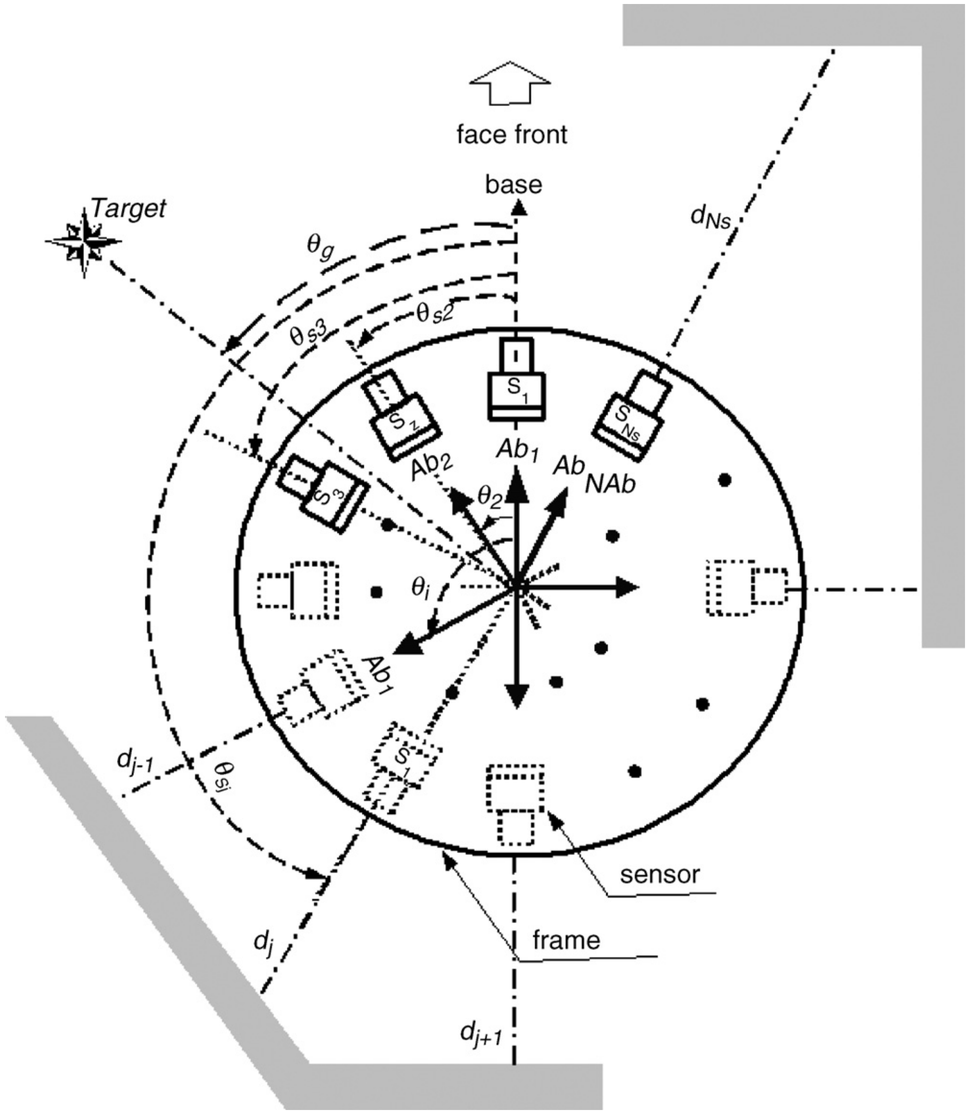

Fig. 4. Configuration of mobile robot and its relatives to target and obstacles.

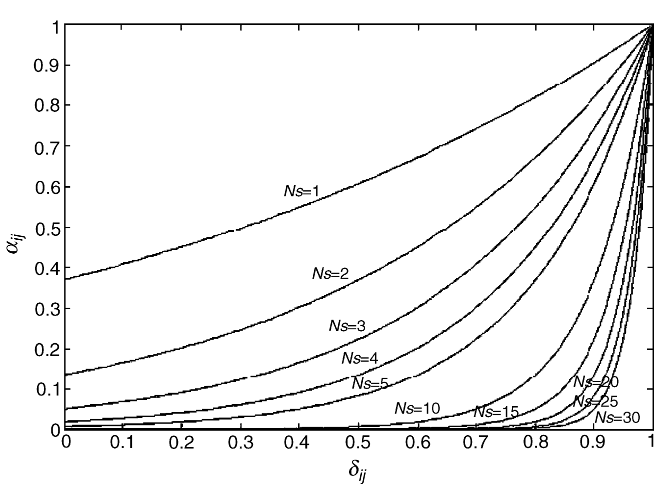

Fig. 5. Relation between α_{ij} and δ_{ij}.

spatial relationship is consistently discriminative between different parts of an environment, and the same representation can be used for different environments. Therefore, this method is tolerant with respect to the environmental changes. The interpreter is regarded as a phagocyte and translates sensor data into perception. The antigen presentation proceeds from the information extraction to the perception translation. An antigen

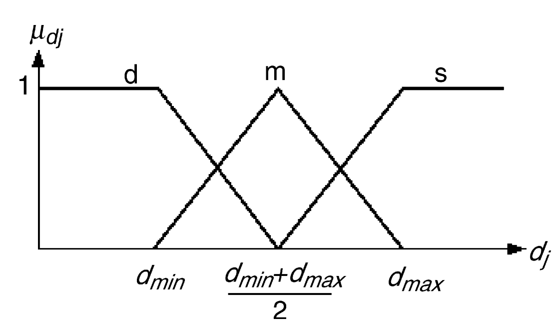

Fig. 6. Membership function and labels for measured distance d_j.

may have several different epitopes, which means that an antigen can be recognized by a number of different antibodies. However, an antibody can bind only one antigen's epitope. In the proposed mechanism, a paratope with a built-in robot's steering direction is regarded as a antibody and interacts with each other and with its environment. These antibodies/steering-directions are induced by recognition of the available antigens/detected-information. In should be noted that only one antibody with the highest concentration will be selected to act according to the immune network hypothesis.

In the proposed immune network, antibodies are defined as the steering directions of mobile robots as illustrated in Fig. 4:

$$\mathrm{Ab}_i \equiv \theta_i = \frac{360^\circ}{N_{\mathrm{Ab}}}(i-1), \quad i = 1, 2, \ldots, N_{\mathrm{Ab}}$$

where N_{Ab} is the number of antibodies/steering-directions and θ_i is the steering angle between the moving path and the head orientation of the mobile robot. Note that $0^\circ \le \theta_i \le 360^\circ$. In addition, the antigen represents the local environment surrounding the robot and its epitopes are a fusion data set

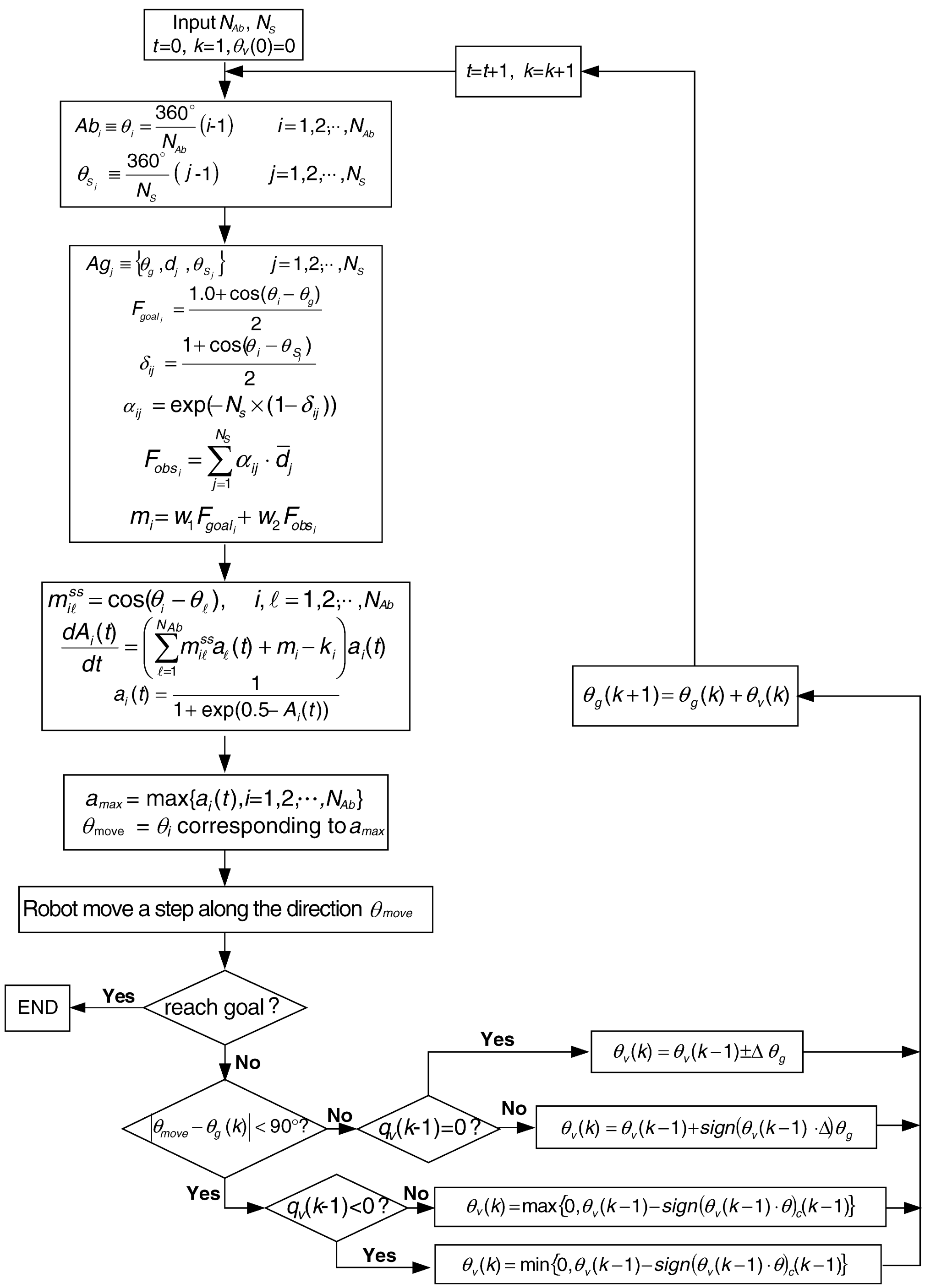

Fig. 7. Flowchart of the mobile robot navigation procedure.

Table 1
Variables used in the reactive immune network

Notation	Description
Ab_i	The ith antibody/steering angle θ_i
Ag_j	The jth antigen/environment state respect to the jth sensor
N_{Ab}	Number of antibodies/steering-directions
θ_i	Steering angle between the moving path and the head orientation of the mobile robot
θ_g	Azimuth of the goal position
d_j	Distance between the obstacles and the jth sensor
θ_{S_j}	Azimuth of the jth sensor
N_s	Number of sensors equally spaced around
m_i	the affinity value between the antigen/local environment and the ith antibody/steering angle
F_{goal_i}	The attractive force of the ith steering direction
F_{obsl_i}	The repulsive force of the ith steering direction
w_1, w_2	Weighting values
α_{ij}	The weighting ratio for the jth sensor/antigen to the ith antibody/steering angle θ_i
δ_{ij}	Coefficient express influence and importance of each sensor at different locations
$\bar{d}_j$	The normalized obstacle distance for each sensor
μ	The matching degree of the corresponding fuzzy rule
m_{ij}^{ss}	The stimulative-suppressive affinity between the ith and jth antibody/steering-angle
m_{ij}^{st}	The stimulative affinity between the ith and jth antibody/steering-angle
m_{ij}^{su}	The suppressive affinity between the ith and jth antibody/steering-angle
θ_v	The virtual robot-to-target angle
θ_c	Converging angle
λ	Adjustable decay angle

containing the azimuth of the goal position θ_g, the distance between the obstacles and the jth sensor d_j, and the azimuth of sensor θ_{S_j}:

$$\theta_{S_j} \equiv \frac{360^\circ}{N_s}(j-1), \quad j = 1, 2, \ldots, N_s,$$

$$Ag_j \equiv \{\theta_g, d_j, \theta_{S_j}\}, \quad j = 1, 2, \ldots, N_s$$

where N_s is the number of sensors equally spaced around the base plate of the mobile robot, $d_{min} \leq d_j \leq d_{max}$ and $0^\circ \leq \theta_{S_j} \leq 360^\circ$. Parameters d_{min} and d_{max} represent the nearest and longest distances measured by the range sensors, respectively. It should be noted that different antigens (local environments) might have identical epitopes (fusion information from range sensors). There is no necessary relationship between N_{Ab} and N_s since they depend on the hardware (*i.e.* motor steering angles and number of sensors installed) of mobile robot. Nevertheless, simulation results show that better performance could be derived if N_s equal to or larger than N_{Ab}.

The potential-field method is one of the most popular approaches employed to navigate the mobile robot within environments containing obstacles, since it is conceptually effective and easy to implement. The method can be implemented either for off-line global planning if the environment is previously known or for real-time local navigation in an unknown environment using onboard sensors. The artificial potential field (APF) approach considers a virtual attractive force between the robot and the target as well as virtual repulsive forces between the robot and the obstacles. The resultant force on the robot is then used to decide the

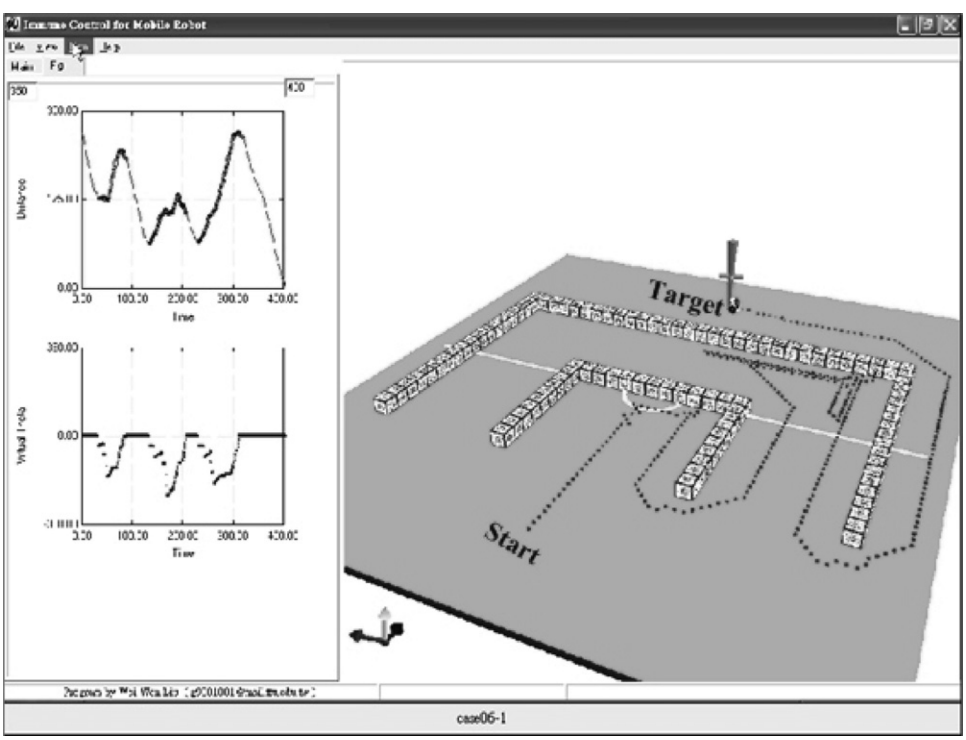

Fig. 8. Simulation window of the mobile robot navigating in a double U-shaped obstacles.

direction of its movements. In the proposed immune network, the resultant force on the robot is defined as m_i, the affinity value between the antigen/local environment and the ith antibody/steering angle:

$$m_i = w_1 F_{\mathrm{goal}_i} + w_2 F_{\mathrm{obs}_i}, \quad i = 1, 2, \ldots, N_{\mathrm{Ab}} \tag{3}$$

The weighing values w_1 and w_2 indicate the ratio between attractive and repulsive forces. Note that $0 \leq w_1, w_2 \leq 1$ and $w_1 + w_2 = 1$. The attractive force F_{goal_i} of the ith steering direction (*i.e.* the ith antibody) is defined as follows:

$$F_{\mathrm{goal}_i} = \frac{1.0 + \cos(\theta_i - \theta_{\mathrm{g}})}{2.0}, \quad i = 1, 2, \ldots, N_{\mathrm{Ab}} \tag{4}$$

Note that F_{goal_i} is normalized and $0 \leq F_{\mathrm{goal}_i} \leq 1$. Obviously, the attractive force is at its maximal level ($F_{\mathrm{goal}_i} = 1$) when the mobile robot goes straightforward to the target (*i.e.* $\theta_i = \theta_{\mathrm{g}}$). On the contrary, it is minimized ($F_{\mathrm{goal}_i} = 0$) if the robot's steering direction is the opposite of the goal.

The repulsive force for each moving direction (the ith antibody θ_i) is expressed as the following equation:

$$F_{\mathrm{obs}_i} = \sum_{j=1}^{N_{\mathrm{s}}} \alpha_{ij} \bar{d}_j, \tag{5}$$

where $\alpha_{ij} = \exp(-N_{\mathrm{s}} \times (1 - \delta_{ij}))$ with $\delta_{ij} = 1 + \cos(\theta_i - \theta_{\mathrm{S}_j})/2$. Fig. 5 demonstrates the relationship between α_{ij} and δ_{ij}. The parameter α_{ij} indicates the weighting ratio for the jth sensor to steering angle θ_i while $\bar{d}_j$ represents the normalized distance between the jth sensor and the obstacles. Coefficient δ_{ij} expresses influence and importance of each sensor at different locations. The equation shows that the information derived from the sensor closest to the steering direction is much more important due to its biggest δ_{ij} value. Kubota et al. [44] have proposed a similar 'delta rule' to evaluate the weighting of each sensor too.

The normalized obstacle distance for each sensor $\bar{d}_j$ is fuzzified using the fuzzy set definitions. The mapping from the fuzzy subspace to the TSK model is represented as three fuzzy if-then rules in the form of

$$\text{IF } \mathrm{d}_j \text{ is s THEN } y = L_1, \qquad \text{IF } \mathrm{d}_j \text{ is m THEN } y = L_2,$$
$$\text{IF } \mathrm{d}_j \text{ is d THEN } y = L_3$$

where L_1, L_2, and L_3 are defined as 0.25, 0.5 and 1.0, respectively. The input variable of each rule is the detected distance d_j of the jth sensor. The antecedent part of each rule has one of the three labels, namely, s (safe), m (medium), and d (danger).

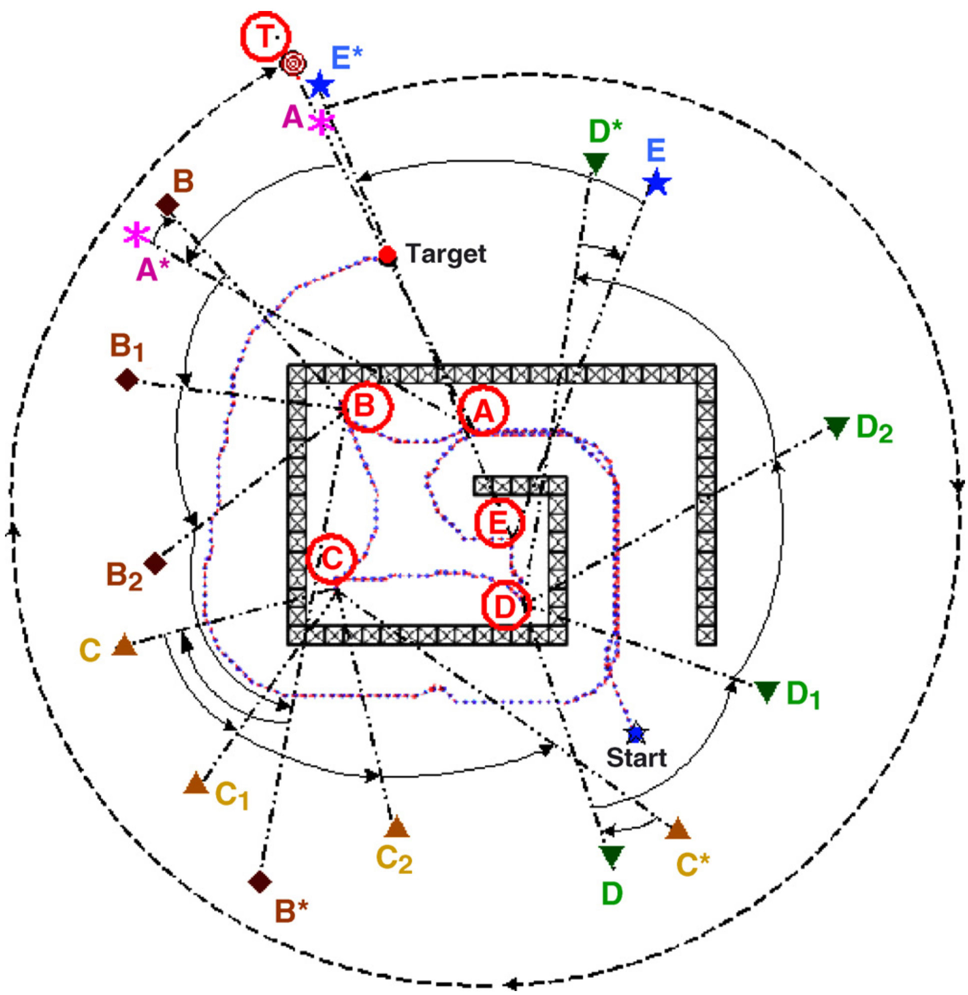

Fig. 9. Robot path and state of the indices along the trajectory.

Consequently, the total output of the fuzzy model is given by the equation below:

$$\bar{d}_j = \frac{\mu_{\mathrm{safe}}(d)L_1 + \mu_{\mathrm{medium}}(d)L_2 + \mu_{\mathrm{danger}}(d)L_3}{\mu_{\mathrm{safe}}(d) + \mu_{\mathrm{medium}}(d) + \mu_{\mathrm{danger}}(d)} \tag{6}$$

where $\mu_{\mathrm{safe}}(d)$, $\mu_{\mathrm{medium}}(d)$, $\mu_{\mathrm{danger}}(d)$ represent the matching degree of the corresponding rule. The inputs to the TSK model are crisp numbers; therefore, the degree of the input matches its rule is and computed using the "min operator". Fig. 6 illustrates the membership function and labels for measured distance d_j.

As to the stimulative–suppressive interaction between the antibodies/steering-directions are derived from Eq. (1) as follows:

$$\begin{aligned}
\frac{\mathrm{d}A_i(t)}{\mathrm{d}t} &= \left(\sum_{\ell=1}^{N_{\mathrm{Ab}}} m_{i\ell}^{\mathrm{st}} a_\ell(t) - \sum_{k=1}^{N_{\mathrm{Ab}}} m_{ki}^{\mathrm{su}} a_k(t) + m_i - k_i\right) a_i(t) \\
&= [(m_{i1}^{\mathrm{st}} a_1(t) + m_{i2}^{\mathrm{st}} a_2(t) + \cdots + m_{iN_{\mathrm{Ab}}}^{\mathrm{st}} a_{N_{\mathrm{Ab}}}(t)) \\
&\quad - (m_{1i}^{\mathrm{su}} a_1(t) + m_{2i}^{\mathrm{su}} a_2(t) + \cdots + m_{N_{\mathrm{Ab}}i}^{\mathrm{su}} a_{N_{\mathrm{Ab}}}(t)) + m_i \\
&\quad - k_i] a_i(t) \\
&= [(m_{i1}^{\mathrm{st}} - m_{1i}^{\mathrm{su}}) a_1(t) + (m_{i2}^{\mathrm{st}} - m_{2i}^{\mathrm{su}}) a_2(t) + \cdots \\
&\quad + (m_{iN_{\mathrm{Ab}}}^{\mathrm{st}} - m_{N_{\mathrm{Ab}}i}^{\mathrm{su}}) a_{N_{\mathrm{Ab}}}(t) + m_i - k_i] a_i(t) \\
&= [m_{i1}^{\mathrm{ss}} a_1(t) + m_{i2}^{\mathrm{ss}} a_2(t) + \cdots + m_{iN_{\mathrm{Ab}}}^{\mathrm{ss}} a_{N_{\mathrm{Ab}}}(t) + m_i \\
&\quad - k_i] a_i(t) \\
&= \left(\sum_{\ell=1}^{N_{\mathrm{Ab}}} m_{i\ell}^{\mathrm{ss}} a_\ell(t) + m_i - k_i\right) a_i(t)
\end{aligned}$$

and the stimulative–suppressive affinity $m_{i\ell}^{\mathrm{ss}}$ between the ith and jth antibody/steering-angle is defined as

$$m_{i\ell}^{\mathrm{ss}} = m_{i\ell}^{\mathrm{st}} - m_{\ell i}^{\mathrm{su}} = \cos(\theta_i - \theta_\ell) = \cos(\Delta\theta_{i\ell}), \quad i, \ell = 1, 2, \ldots, N_{\mathrm{Ab}} \tag{7}$$

the highest concentration is selected to activate its corresponding behavior to the world. Therefore, mobile robot moves a step along the direction of the chosen steering angle/antibody.

4. Local minimum recovery

As mentioned in the previous section, one problem inherent in the APF method is the possibility for the robot to get trapped in a local minima situation. Traps can be created by a variety of obstacle configurations. The key issue to the local minima problems is the detection of the local minima situation during the robot's traversal. In this study, the comparison between the robot-to-target direction θ_{g} and the actual instantaneous direction of travel θ_i was utilized to detect if the robot got trapped. The robot is very likely to get trapped and starts to move away from the goal if the robot's direction of travel is more than 90° off-target (*i.e.* $|\theta_i - \theta_{\mathrm{g}}| > 90°$). Various approaches for escaping trapping situations have been proposed as described previously. In this study, an adaptive virtual target method is developed and integrated with the reactive immune network to guide the robot out of the trap.

In immunology, the T-cell plays a remarkable key role in distinguishing a "self" from other "non-self" antigens. The Helper T-cells work primarily by secreting substances to constitute powerful chemical messengers to promote cellular growth, activation and regulation. Simulating the biological immune system, this material can either stimulate or suppress the promotion of antibodies/steering-directions depending on whether the antigen is non-self or self (trapped in local minima or not). Different from the virtual target method proposed in [10,11], an additional virtual robot-to-target angle θ_{v} (analogous to the interleukine secreted by T-cells) is added to the goal angle θ_{g} whenever the trap condition ($|\theta_i - \theta_{\mathrm{g}}| > 90°$) is satisfied:

$$\theta_{\mathrm{g}}(k+1) = \theta_{\mathrm{g}}(k) + \theta_{\mathrm{v}}(k) \tag{8}$$

with

$$\begin{cases}
\theta_{\mathrm{v}}(k) = \theta_{\mathrm{v}}(k-1) \pm \Delta\theta_{\mathrm{g}} & \text{if } |\theta_i(k) - \theta_{\mathrm{g}}(k)| \geq 90° \text{ and } \theta_{\mathrm{v}}(k-1) = 0 \\
\theta_{\mathrm{v}}(k) = \theta_{\mathrm{v}}(k-1) + \mathrm{sign}(\theta_{\mathrm{v}}(k-1))\Delta\theta_{\mathrm{g}} & \text{if } |\theta_i(k) - \theta_{\mathrm{g}}(k)| \geq 90° \text{ and } \theta_{\mathrm{v}}(k-1) \neq 0 \\
\theta_{\mathrm{v}}(k) = \max\{0, \theta_{\mathrm{v}}(k-1) - \mathrm{sign}(\theta_{\mathrm{v}}(k-1))\theta_{\mathrm{c}}(k-1)\} & \text{if } |\theta_i(k) - \theta_{\mathrm{g}}(k)| < 90° \text{ and } \theta_{\mathrm{v}}(k-1) \geq 0 \\
\theta_{\mathrm{v}}(k) = \min\{0, \theta_{\mathrm{v}}(k-1) - \mathrm{sign}(\theta_{\mathrm{v}}(k-1))\theta_{\mathrm{c}}(k-1)\} & \text{if } |\theta_i(k) - \theta_{\mathrm{g}}(k)| < 90° \text{ and } \theta_{\mathrm{v}}(k-1) < 0
\end{cases}$$

Obviously, stimulative–suppressive effect is positive ($m_{i\ell}^{\mathrm{ss}} > 0$) if $-90° < \Delta\theta_{i\ell} < 90°$. On the contrary, negative stimulative–suppressive effect exists between two antibodies if their difference of steering angles are greater than 90° or less than −90° (*i.e.*, $\Delta\theta_{i\ell} > 90°$ or $\Delta\theta_{i\ell} < -90°$). In addition, there is no any net effect between orthogonal antibodies (*i.e.* $\Delta\theta_{i\ell} = \pm 90°$). The immune system responses to the specified winning situation that has the maximum concentration among the trigged antibodies by comparing the currently perceived situations (trigged antibodies). In other words, antibody with

where $\Delta\theta_{\mathrm{g}} = \theta_{\mathrm{g}}(k) - \theta_{\mathrm{g}}(k-1)$ and $\theta_{\mathrm{c}}(k) = \theta_{\mathrm{c}}(k-1) + \lambda$.

Parameters $k-1$, k, and $k+1$ represent the previous state, the current state and the future state, respectively. Symbol "±" indicates that the location of the virtual target can be randomly switched to either the right (*i.e.* " + ") or the left (*i.e.* "−") side of the mobile robot so that the robot has a higher probability of escaping from the local minima in either direction. λ is an adjustable decay angle. The bigger the value is, the faster the location of virtual target converges to that of the true one and the easier it is for the robot to get trapped in the local minima again. In this study, λ is determined after multiple simulation runs and set to 0.2. The incremental virtual angle $\theta_v(k)$ in the proposed scheme is state dependent and self-adjustable according to the robot's current state and the action it took previously. This provides powerful and effective trap-escaping capability compared to virtual target method, which keeps θ_v a constant value. θ_c is a converging angle and its initial value is 0. Fig. 7 demonstrates the flowchart of navigation procedure for mobile robot employing the proposed reactive immune network; corresponding variables utilized are tabulated in Table 1.

For carrying out the necessary simulation and validating the efficacy of the proposed methodology, a computer program was developed using C++ language with graphical user interface. The simulation environment contains a robot and obstacle constructed by numerous square blocks 10 cm in length. The environmental condition adopted in simulation is a 300 cm × 300 cm grid. The size of the simulated robot is a circle with 10cm diameter. During each excursion, the robot tries to reach target and avoid collision with obstacle. Fig. 8 illustrates the simulation window of the mobile robot navigating in a double U-shaped obstacles and its resulting trajectory. A more detailed description of the proposed scheme and some practical consideration are elaborated in the following example.

Fig. 9 elucidates and demonstrates the performance of the proposed strategy for the robot to escape from a recursive U-trap situation, which may make the virtual target switching strategy [10,11] ineffective as Chatterjee and Matsuno [12] suggested. The robot first enters a U-shaped obstacle and is attracted to the target due to the target's reaching behavior until it reaches the critical point A. The variation of the distance between the target and the corresponding orientation of the virtual target over time is shown in Fig. 10. Clearly, the azimuth of goal θ_g is kept the same during this stage; however, the distance between the robot and the target is decreased quickly. The detection of the trap possibility because of the abrupt change of target orientation at location A (θ_g) makes the target shift to a virtual position A^* ($\theta_g - \Delta\theta_g$). $\Delta\theta_g$ is defined as 45° is this study. Note that the switch-to-left or the switch-to-right of the virtual target (*i.e.*, minus or plus $\Delta\theta_g$) is selected randomly. On the way A → B, $\Delta\theta_g$ is decreased gradually according to Eq. (8) until a new local minimal is found at location B. Again, the location of virtual target switches from A^* to B^*. Figs. 9 and 10 show that there is a successive virtual target switching $A^* \rightarrow B_1 \rightarrow B_2 \rightarrow B^*$ when the robot moves around the left upper corner where it is tracked in a trap (to satisfy condition $|\theta_i - \theta_g| > 90°$) three times. After passing through the critical point B, the robot keeps approaching the virtual target until reaching the third critical point C. Concurrently, the associated orientation of the virtual target is decreased from B^* to C. Once more, it takes three times for the robot to escape from the trap situation in the left lower corner on the path C → D (orientation of the virtual target $C \rightarrow C_1 \rightarrow C_2 \rightarrow C^* \rightarrow D$). Similar navigation procedures take place on the way D → E (orientation of virtual target $D \rightarrow D_1 \rightarrow D_2 \rightarrow D^* \rightarrow E \rightarrow E^*$). After escaping from the recursive U-shaped trap, the mobile robot revolves in a circle and finally reaches target T without any trapping situations (azimuth of virtual target θ_g decreases gradually from E^* to T illustrated with a dashed line). The derived trajectory

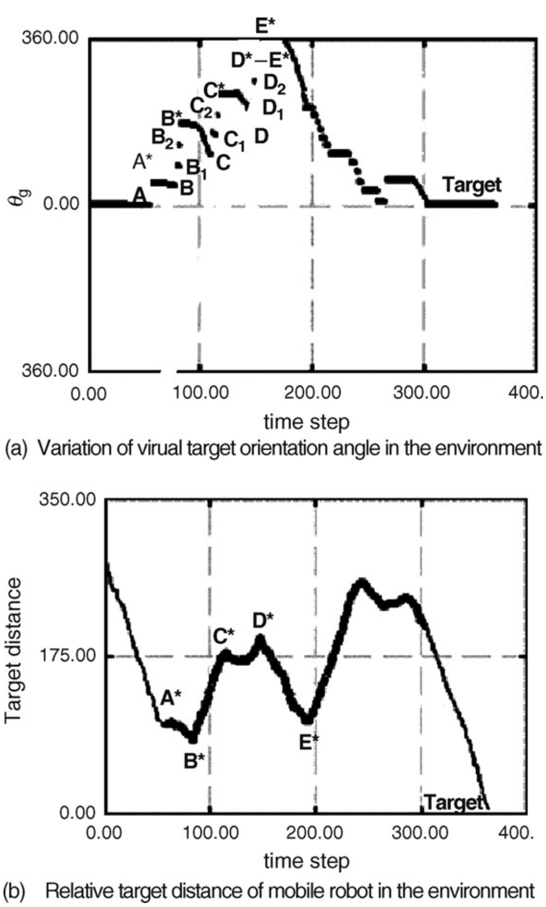

Fig. 10. Variation of virtual target orientation and relative distance of mobile robot.

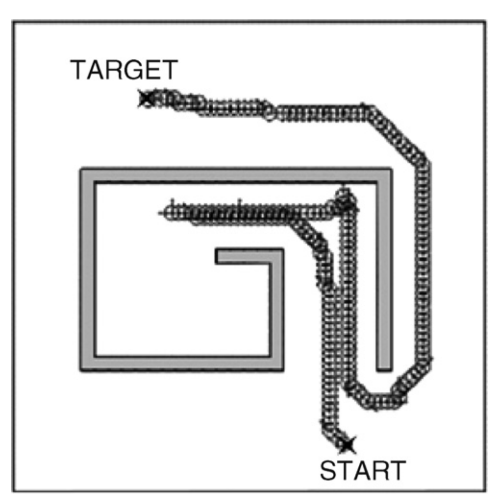

Fig. 11. The other possible trajectories to escape the recursive trap situation.

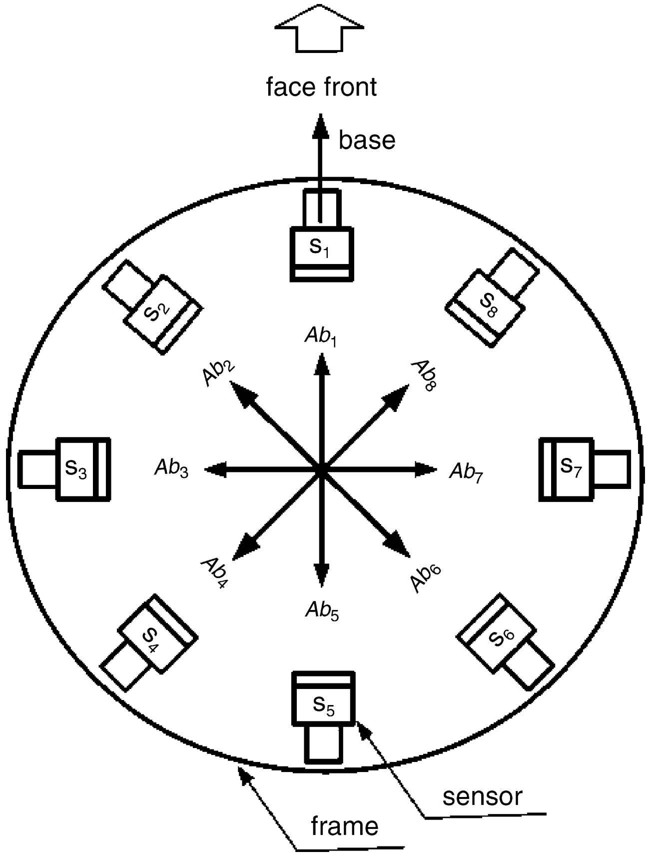

Fig. 12. Configuration of mobile robot employed in simulation.

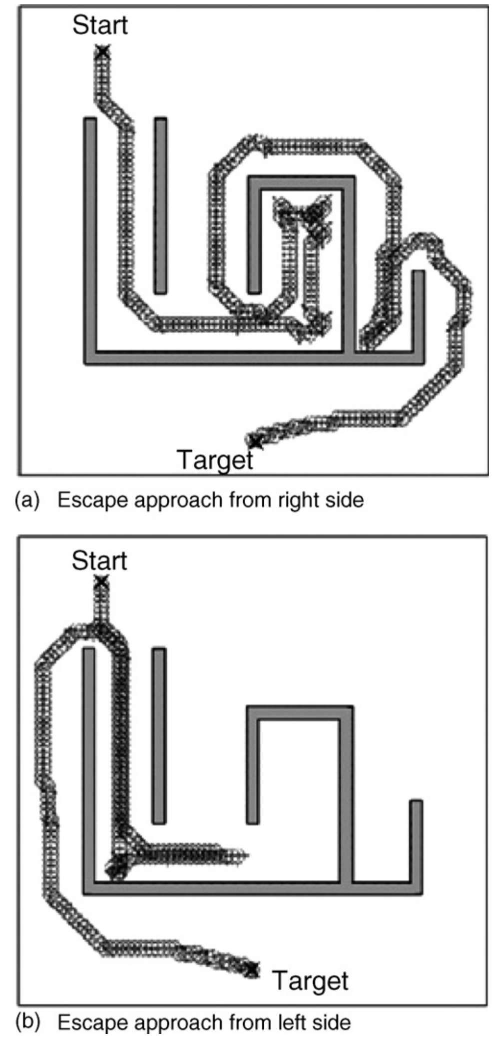

Fig. 13. Robot trajectories to escape from loop type and dead-end type trap situation.

illustrated in Fig. 9 is quite similar to the results derived by Chatterjee and Matsuno [12]. Fig. 11 illustrates the other possible trajectory to escape the same trap situation due to the random choice of the ''plus'' or ''minus'' robot-to-target angle $\Delta\theta_g$, as shown in Eq. (8). Obviously, the mechanism for virtual target switching to the right or to the left (*i.e.*, $\pm\Delta\theta_g$) increases the diversity and possibility of the robot's escaping from the local minima problem.

5. Simulation and discussions

Numerous simulation examples presented by researchers [10,12,44] were conducted to demonstrate the performance of mobile robot navigation employing RIN to various unknown environments; in particular, the capability of escaping from the traps or the wandering situations described. Assuming that the robot has eight uniformly distributed distance sensors (*i.e.* $N_s = 8$) and eight moving directions including forward, left, right, back, forward left, forward right, back left, and back right (*i.e.* $N_{Ab} = 8$) as Fig. 12 shows. Fig. 13(a) demonstrates the similar trajectory of the mobile robot to escape from loop-type and dead-end-type trapping situations in [12]. Again, Fig. 13(b) demonstrates the other possible trajectory (escaping from the left side) due to the random selection scheme (''±'') mentioned previously. To validate the efficiency of the proposed scheme further, three trap environments adopted in [45] were utilized in this study. Obviously, the simulation results depicted in Fig. 14 show that the robot is capable of escaping from all the traps as expected. Moreover, to demonstrate the flexibility and effectiveness of the proposed methodology, both the number of sensors/antigens and steering angles/antibodies are reduced to one half. Four sensors are placed uniformly at 0°, 90°, 180°, 270°, and the four steering directions are forward, right, left, and back. The trajectories of mobile robots at the same environments as Fig. 15 illustrated validate the performance of the proposed strategy even using a simpler configuration (less sensors and steering angles).

Finally, the most famous and utilized example in mobile robot navigation, U-shaped trap problem, is employed in this study. Fig. 16 shows part of the paths of the robot escaping from the U-shaped trap with different *L*/*W* (length/width) ratios. Apparently, the robot is capable of escaping from different ratio U-shaped environments. As to the double U-shaped trap environment [44], Fig. 17 demonstrates the four trajectories for the robot to escape utilized RIN. Apparently, RIN successfully drives the robot to escape the double U-shaped trap.

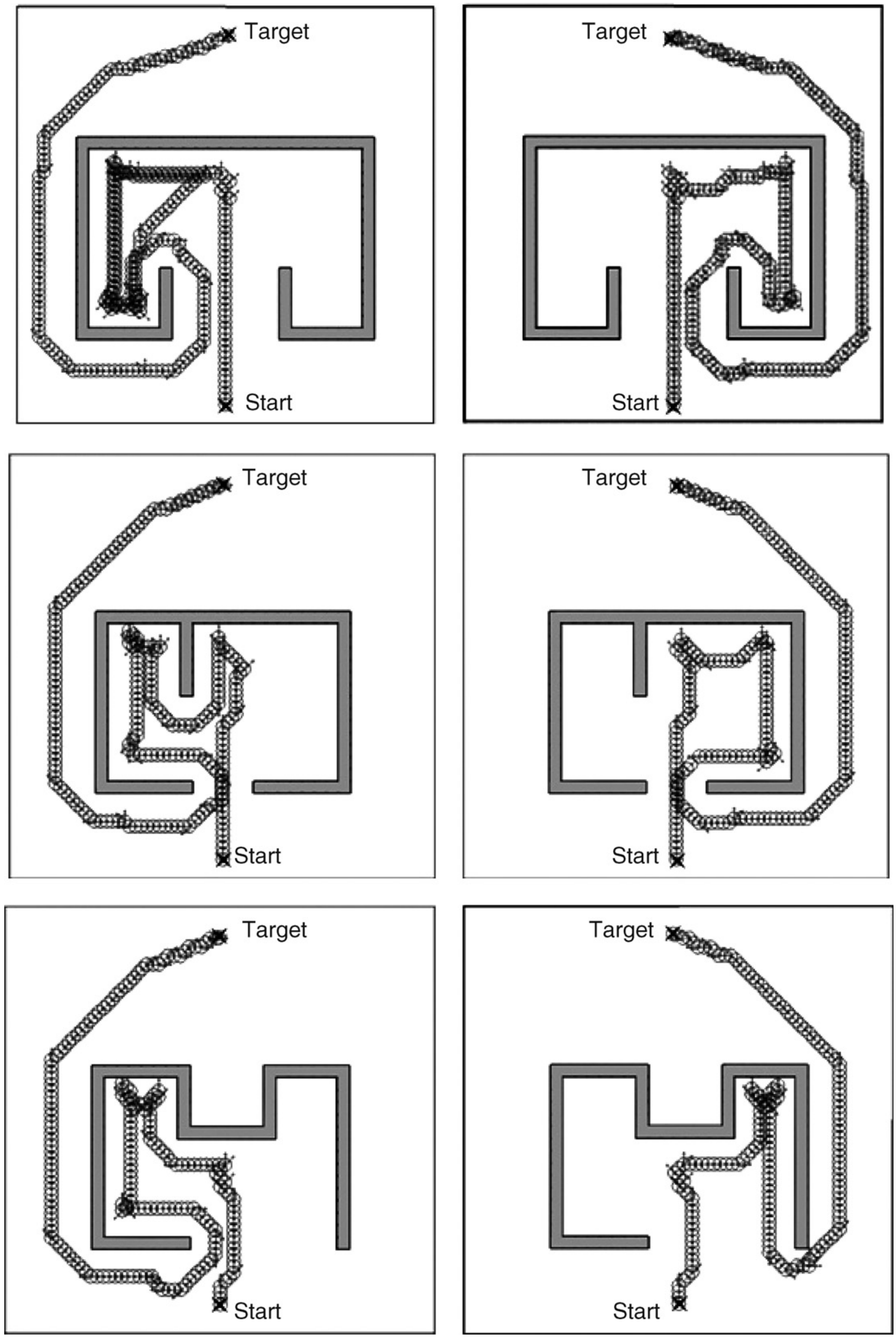

Fig. 14. Robot trajectories to escape from different trapping situations.

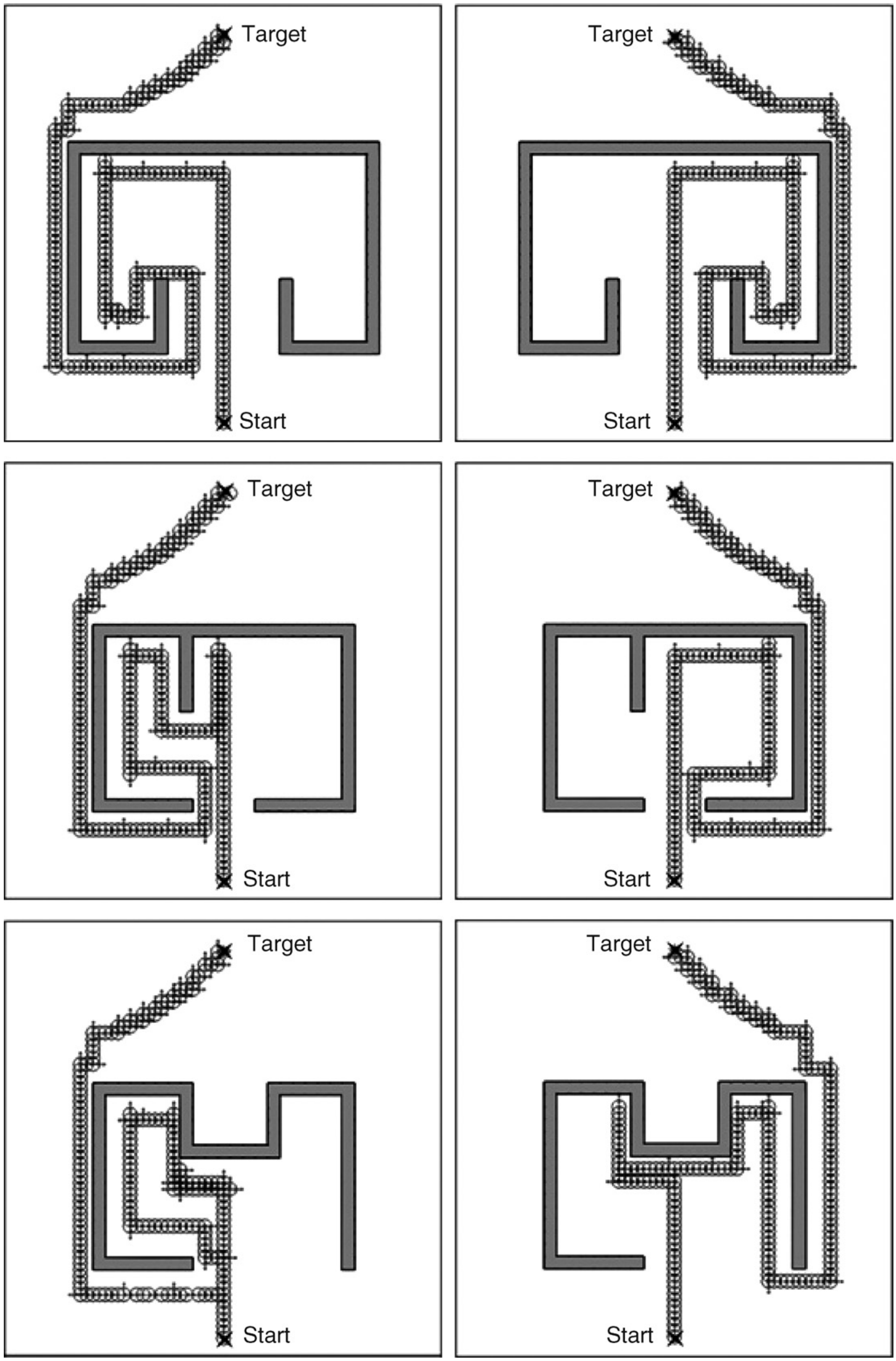

Fig. 15. Robot trajectories to escape the same trapping situations with simpler architecture.

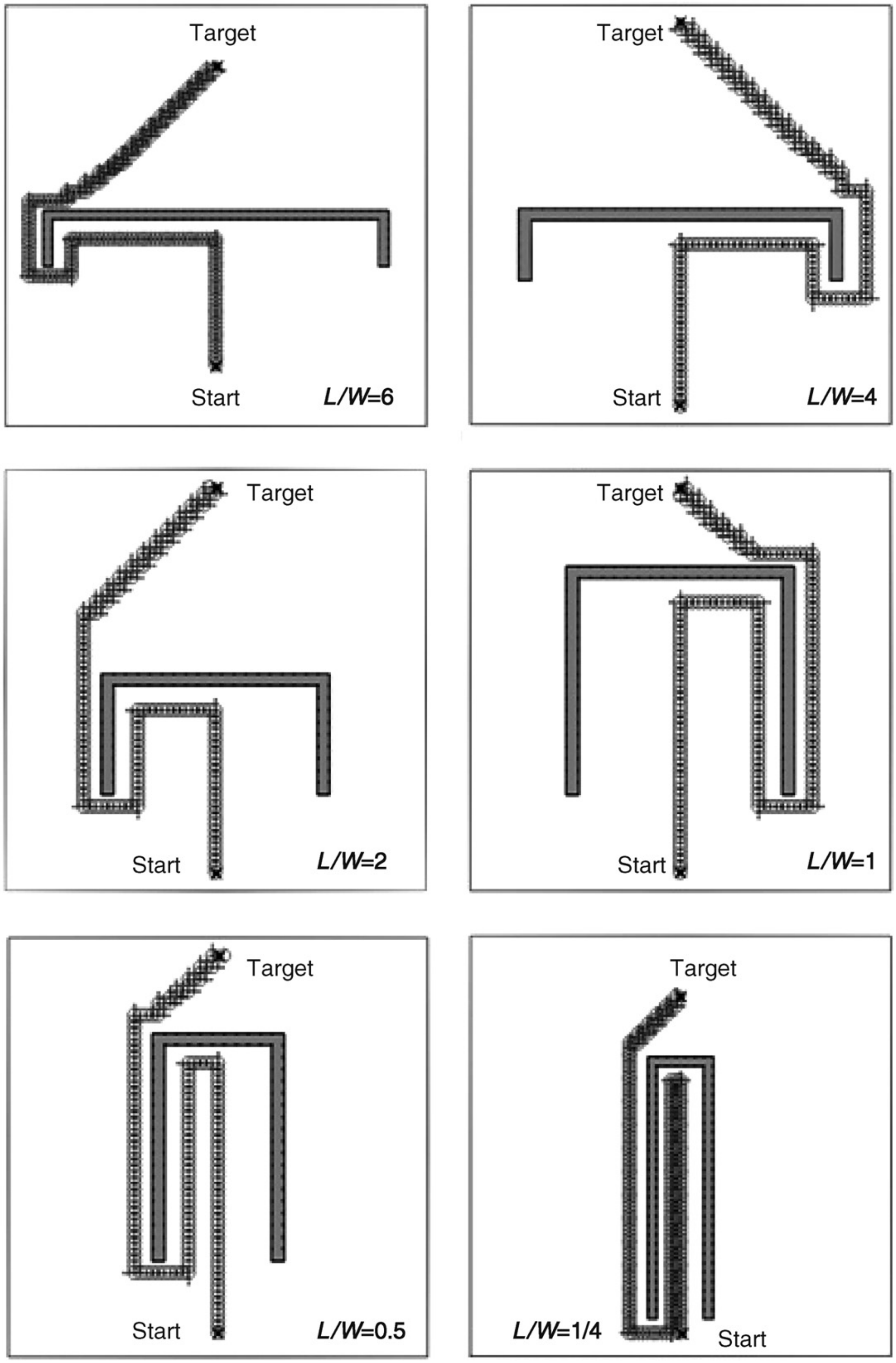

Fig. 16. Robot trajectories to escape from U-shaped trap with different length/width ratio.

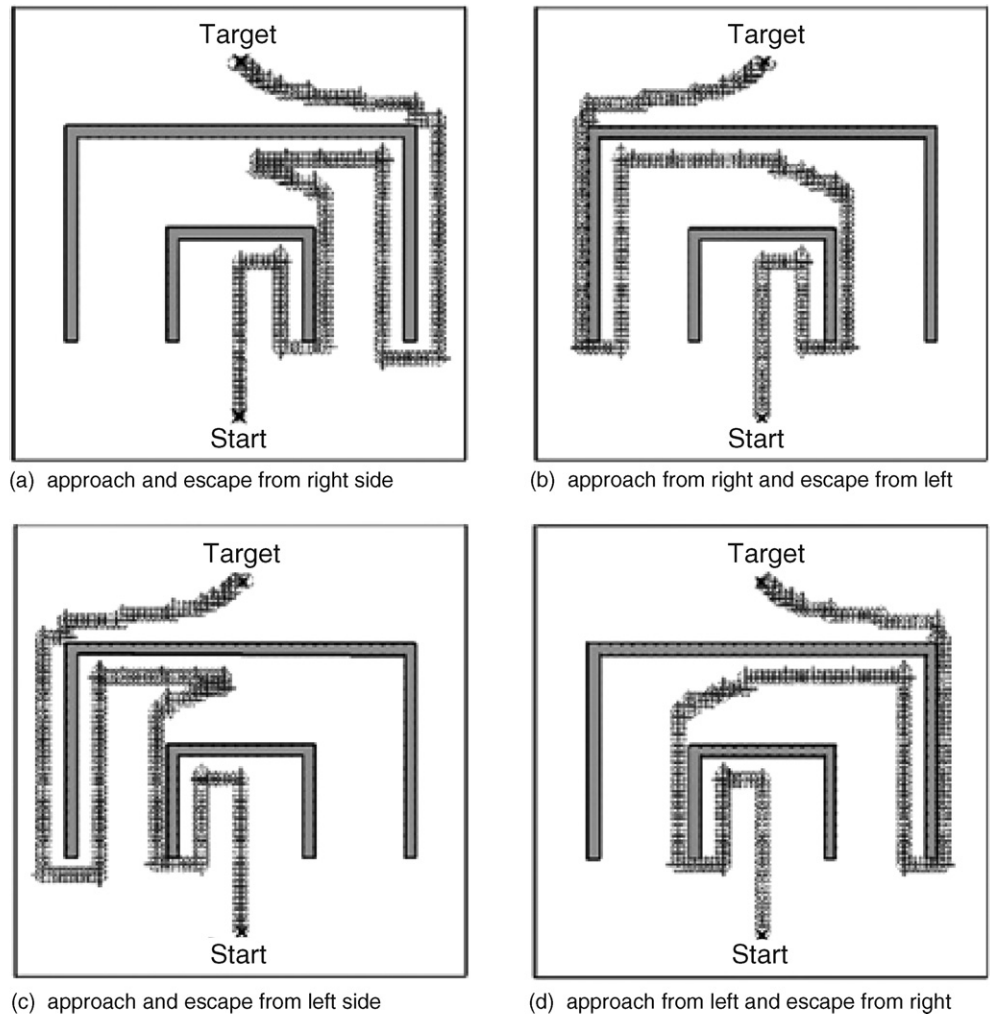

Fig. 17. Robot trajectories to escape from double U-shaped trap.

6. Conclusions

A reactive immune network inspired by the biological immune system is developed for mobile robot navigation. In addition, an adaptive virtual target method is integrated to solve the local minima problem. Several trap environments employed in early studies are employed to evaluate the performance of the proposed methodology. Simulation results validate the flexibility, efficiency and effectiveness of the robot navigation architecture, especially the solution of the local minima problem. Currently, an omni-directional mobile robot with 12 ultrasonic sensors and two cameras is set up to evaluate RIN's perspective applications experimentally. Besides, the developed architecture is modified presently solving the moving-obstacles problem.

Acknowledgment

The authors would like to acknowledge the National Science Council, Taiwan, for making this work possible with Grant NSC94-2213-E-036-002.

References

[1] O. Khatib, Real-time obstacle avoidance for manipulators and mobile robot, Int. J. Robotic Res. 5 (1) (1986) 90–99.
[2] J.C. Latombe, Robot Motion Planning, Kluwer Academic Publishers, Dordrecht, 1991.
[3] J. Baraquand, J.C. Latombe, A Monte-Carlo algorithm for path planning with many degrees of freedom, in: Proceedings of the IEEE International Conference on Robotics and Automation, Cincinnati, OH, (1990), pp. 1712–1717.
[4] H. Chang, A new technique to handle local minima for imperfect potential field based motion planning, in: Proceedings of the IEEE International Conference on Robotics and Automation, Minneapolis, MN, (1996), pp. 108–112.
[5] S. Lee, T.M. Adams, B.-Y. Ryoo, A fuzzy navigation system for mobile construction robots, Automat. Construct. 6 (1997) 97–107.
[6] J. Borenstein, Y. Koren, Real-time obstacle avoidance for fast mobile robots, IEEE Trans. Syst. Man Cybernet. 9 (5) (1989) 1179–1197.
[7] X. Yun, K.-C. Tan, A wall-following method for escaping local minima in potential field based motion planning, in: Proceedings of the IEEE International Conference on Robotics and Automation, Monterey, CA, (1997), pp. 421–426.
[8] C. Liu, H.A. Marcelo Jr., K. Hariharan, S.Y. Lim, Virtual obstacle concept for local-minimum-recovery in potential-field based navigation,

in: Proceedings of the IEEE International Conference on Robotics and Automation, San Francisco, CA, (2000), pp. 983–988.

[9] M.G. Park, M.C. Lee, Artificial potential field based path planning for mobile robots using a virtual obstacle concept, in: Proceedings of the IEEE/ASME International Conference on Advanced Intelligent Mechatronics, 2003, pp. 735–740.

[10] W.L. Xu, A virtual target approach for resolving the limit cycle problem in navigation of a fuzzy behaviour-based mobile robot, Robotics Autonom. Syst. 30 (2000) 315–324.

[11] W.L. Xu, S.K. Tso, Y.H. Fung, Fuzzy reactive control of a mobile robot incorporating a real/virtual target switching strategy, Robotics Autonom. Syst. 23 (1998) 171–186.

[12] R. Chatterjee, F. Matsuno, Use of single side reflex for autonomous navigation of mobile robots in unknown environments, Robotics Autonom. Syst. 35 (2001) 77–96.

[13] D. Dasgupta, Artificial Immune Systems and Their Applications, Springer-Verlag, Berlin Heidelberg, 1999.

[14] L.N. de Castro, T. Jonathan, Artificial Immune Systems: A New Computational Intelligence Approach, Springer-Verlag, 1999.

[15] L.N. de Castro, F.J. Von Zuben, Artificial immune systems. Part I. Basic theory and applications. Technical Report TR-DCA 01/99, 1999.

[16] L.N. de Castro, F.J. Von Zuben, Artificial immune systems. Part II. A survey of applications. Technical Report TR-DCA 02/00, 1999.

[17] Y. Ishida, The immune system as a prototype of autonomous decentralized systems: an overview, in: Proceedings of the Third International Symposium on autonomous decentralized systems, 1997, pp. 85–92.

[18] G.-C. Luh, W.-C. Cheng, Behavior-based intelligent mobile robot using immunized reinforcement adaptive learning mechanism, Adv. Eng. Informat. 16 (2) (2002) 85–98.

[19] E. Hart, P. Ross, A. Webb, A. Lawson, A role for immunology in "next generation" robot controllers, Lecture Notes Comput. Sci. 2787 (2003) 46–56.

[20] A. Ishiguro, T. Kondo, Y. Watanabe, Y. Uchikawa, Dynamic behavior arbitration of autonomous mobile robots using immune networks, in: IEEE International Conference on Evolutionary Computation, Perth, Australia, (1995), pp. 722–727.

[21] A. Ishiguro, Y. Shirai, T. Kondo, Y. Uchikawa, Immunoid: an architecture for behavior arbitration based on the immune networks, in: Proceedings of the IEEE/RSJ International Conference on Intelligent Robots and Systems, Osaka, Japan, (1996), pp. 1730–1738.

[22] A. Ishiguro, Y. Watanabe, T. Kondo, Y. Uchikawa, Decentralized consensus-making mechanisms based on immune system, in: Proceedings of the IEEE International Conference on Evolutionary Computation, Nayoya, Japan, (1996), pp. 82–87.

[23] A. Ishiguro, T. Kondo, Y. Watanabe, Y. Shirai, Y. Uchikawa, Emergent construction of artificial immune networks for autonomous mobile robots, in: Proceedings of the IEEE International Conference on Systems, Man, and Cybernetics, Orlando, Florida, (1997), pp. 1222–1228.

[24] R. Michelan, J.V. Fernando, Decentralized control system for autonomous navigation based on an evolved artificial immune network, in: Proceedings of the IEEE World Congress on Computational Intelligence, Honolulu, Hawaii, (2002), pp. 1021–1026.

[25] H. Meshref, H. VanLandingham, Artificial immune systems: application to autonomous agents, in: Proceedings of the IEEE International Conference on Systems, Man, and Cybernetics, Nashville, TN, (2000), pp. 61–66.

[26] Q.J. Duan, R.X. Wang, H.S. Feng, L.G. Wang, Applying synthesized immune networks hypothesis to mobile robots, in: Proceedings of the IEEE International Conference on Autonomous Decentralized Systems, Chengdu, CHN, (2005), pp. 69–73.

[27] S.M. Thayer, P.N. Singh, Development of an immunology-based multi-robot coordination algorithm for exploration and mapping domains, in: Proceedings of the IEEE/RSJ International Conference on Intelligent Robots and Systems, Lausanne, Switzerland, (2002), pp. 2735–2739.

[28] D.-W. Lee, K.-B. Sim, Artificial immune network-based cooperative control in collective autonomous mobile robots, in: Proceedings of the IEEE International Workshop on Robot and Human Communication, 1997, pp. 58–63.

[29] J.H. Jun, D.-W. Lee, K.-B. Sim, Realization of cooperative strategies and swarm behavior in distributed autonomous robotics systems using artificial immune system, in: Proceedings of the IEEE International Conference on Systems, Man, and Cybernetics, Tokyo, Japan, (1999), pp. 614–619.

[30] A. Ishiguro, Y. Watanabe, Y. Uchikawa, An immunological approach to dynamic behavior control for autonomous mobile robots, in: Proceedings of the IEEE/RSJ International Conference on Intelligent Robots and Systems, Pittsburg, PA, (1995), pp. 495–500.

[31] D.-J. Lee, M.-J. Lee, Y.-K. Choi, S. Kim, Design of autonomous mobile robot action selector based on a learning artificial immune network structure, in: Proceedings of the Fifth Symposium on Artificial Life and Robotics, Oita, Japan, (2000), pp. 116–119.

[32] P.A. Vargas, L.N. de Castro, R. Michelan, F.J. Von Zuben, Implementation of an Immuno-Gentic Network on a Real Khepera II Robot, in: Proceedings of the IEEE Congress on Evolutionary Computation, Canberra, Australia, (2003), pp. 420–426.

[33] Q.J. Duan, R.X. Wang, H.S. Feng, L.G. Wang, An immunity algorithm for path planning of the autonomous mobile robot, in: Proceedings of the IEEE Eighth International Multitopic Conference, Lahore, Pakistan, (2004), pp. 69–73.

[34] I. Roitt, J. Brostoff, D.K. Male, Immunology, 5th ed., Mosby International Limited, 1998.

[35] M.L. Oprea, Antibody repertories and pathogen recognition: the role of germline diversity and somatic hypermutation, PhD Dissertation, Department of Computer Science, The University of New Mexico, Albuquerque, New Mexico, 1996.

[36] J. Carneiro, A. Coutinho, J. Faro, J. Stewart, A model of the immune network with B-T cell co-operation I-prototypical structures and dynamics, J. Theor. Biol. 182 (1996) 513–529.

[37] D. Dasgupta, Artificial neural networks and artificial immune systems: similarities and differences, in: Proceedings of the IEEE International Conference on Systems, Man, and Cybernetics, Orlando, Florida, (1997), pp. 873–878.

[38] N.K. Jerne, The immune system, Sci. Am. 229 (1) (1973) 52–60.

[39] G.W. Hoffmann, The immune system: a neglected challenge for network theorists, in: Proceedings of the IEEE International Symposium on Circuits and Systems, 1989, pp. 1620–1623.

[40] J.D. Farmer, N.H. Packard, A.S. Perelson, The immune system adaptation, and machine learning, Physica D 22 (1986) 184–204.

[41] G.W. Hoffmann, The immune system: a neglected challenge for network theorists, in: Proceedings of the IEEE International Symposium on Circuits and Systems, 1989, pp. 1620–1623.

[42] J. Carneiro, A. Coutinho, J. Faro, J. Stewar, A model of the immune network with B–T cell co-operation. I. Prototypical structures and dynamics, J. Theor. Biol. 182 (1996) 513–529.

[43] J. Carneiro, A. Coutinho, J. Faro, J. Stewar, A model of the immune network with B-T cell co-operation. II. The simulation of ontogenesis, J. Theor. Biol. 182 (1996) 513–529.

[44] N. Kubota, T. Morioka, F. Kojima, T. Fukuda, Learning of mobile robots using perception-based genetic algorithm, Measurement 29 (2001) 237–248.

[45] K. Madlhava, P.K. Kalra, Perception and remembrance of the environment during real time navigation of a mobile robot, Robotics Autonom. Syst. 37 (2001) 25–51.